Noninvasive Ultrasound Measurements of Temperature Distribution in Solids

Mikhail Skliar

THE UNIVERSITY OF UTAH

1

Ultrasound Temperature Measurements

- SOS is temperature dependent in gases, liquids, and solids: $c=f(T)$.
- SOS can be obtained by measuring TOF of the US pulse:

$$c=\frac{2L}{t_{of}}$$

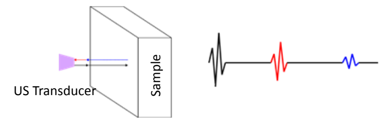

- For the uniform temperature: $T=f^{-1}\left(\frac{2L}{t_{of}}\right)$
- Applications
  - Insertion sensors is difficult or impossible to use
  - Extreme environments
  - Optical measurements not possible

Refractory Degradation

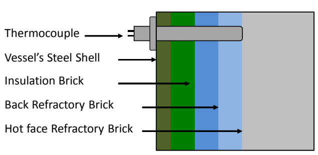

Initial Installation

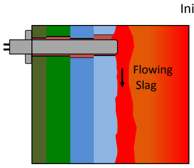

During Gasification

- Slag corrosion
- Mechanical shear
- Refractory liner wear

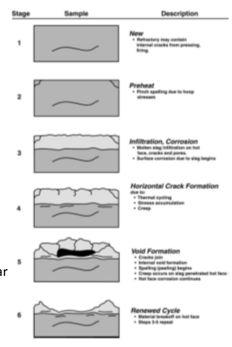

Stages of refractory degradation [1].

3

Commercial Temperature Measurement

- Hardened sensors can withstand harsh environment longer
  - Heavy sheathing makes such devices less sensitive to dynamic changes in temperatures

NETL, DOE

Prof. Zhang Jiansheng: "Domestic TC survive ~1-2 weeks; Rosemount sapphire TC: ~4-6 weeks"

4

Ultrasound Temperature Measurements

- Key difficulty: ***When temperature changes along the path of US propagation***, the acoustic TOF measurements depend on temperature distribution in a complex way:

$$t_{of}=\int_0^L \frac{2}{f\left(T(t,z)\right)}dz$$

Deconvolution of the TOF measurement is an ill-posed problem.

- Parameterizations
  - Assumption that temperature is constant:

$$\int_0^L \frac{2}{f\left(T(z)\right)}dz=\frac{2L}{f(T_o)}$$

  - Linear temperature distribution
  - Heat transfer model

5

Deconvolution of TOF Measurements

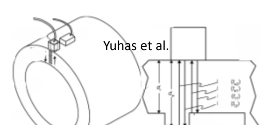

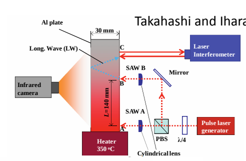

- Use heat transfer model
- Use multiple transducers/receivers

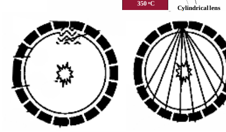

- Produce multiple US echoes

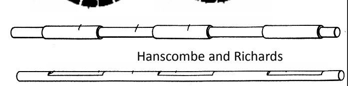

Direct US Measurements of Temperature Distribution

- Create multiple partial reflections that give information about temperature distribution in different segments of the propagation path

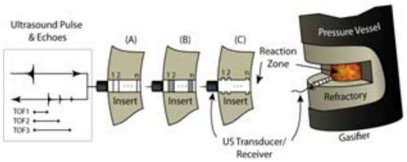

- Methods to create partial reflections:
  - Change in US impedance
  - Scatterers
  - Change in geometry

M. Skliar, K. Whitty, and A. Butterfield, Ultrasonic temperature measurement device, US Patent 8,801,277 B2, 2014.

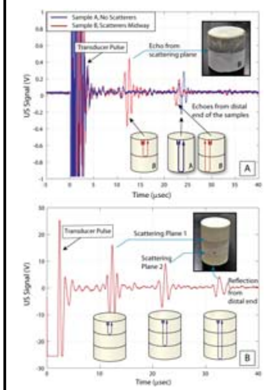

- A: Steel shots were embedded as ultrasound scatters to produce partial reflection at the midpoint of ultrasound propagation path
- B: Two internal interfaces obtained by sequentially casting three layer of identical formulation and allowing for a partial curing before casting the next layer

8

Experimental Setup

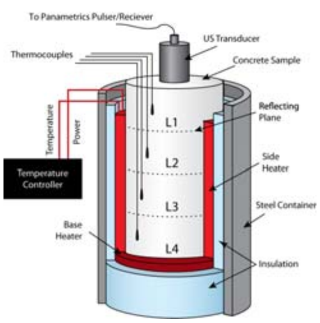

- 4" cementitious sample with four layers
- Surface temperature measured by TCs attached in the middle of each layer

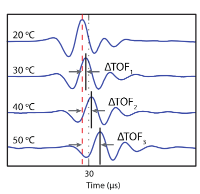

9

Dissipative samples: Accurate timing is difficult

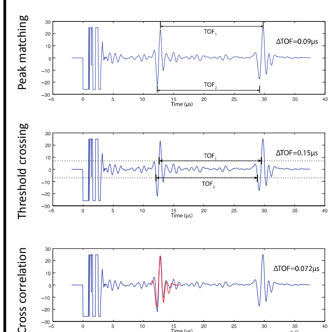

Standard timing techniques

- Single-point features
  - Zero or threshold crossing
  - Peak value
- Shape matching
  - By cross correlation

$$t_{of} = \arg[\max(x(\tau))]$$
$$x(\tau) = \int s_R(t) \cdot s_T(t-\tau)dt$$

  - By minimizing norms

$$t_{of} = \arg[\min(L(\tau))]$$
$$L_1(\tau) = \int |s_R(t) - s_T(t-\tau)|dt$$
$$L_2(\tau) = \int [s_R(t) - s_T(t-\tau)]^2 dt$$

  - Maximizing likelihood

10

Envelope of Ultrasound Waveform

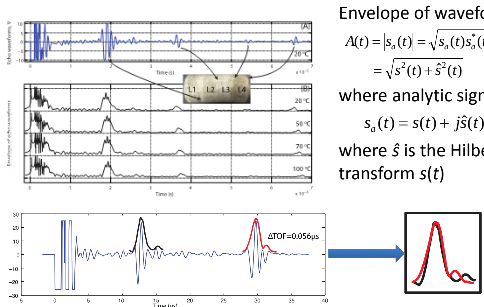

Envelope of waveform

$$A(t) = |s_a(t)| = \sqrt{s_a(t)s_a^*(t)}$$
$$= \sqrt{s^2(t) + \hat{s}^2(t)}$$

where analytic signal

$$s_a(t) = s(t) + j\hat{s}(t)$$

where $\hat{s}$ is the Hilbert transform $s(t)$

11

SOS vs. Temperature Calibration Curve

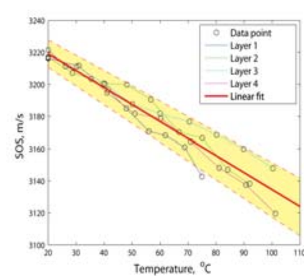

- Linear fit SOS = SOS(T) is based on data for all four layers
- Shaded area shows 95% confidence interval

12

Non-uniform distribution

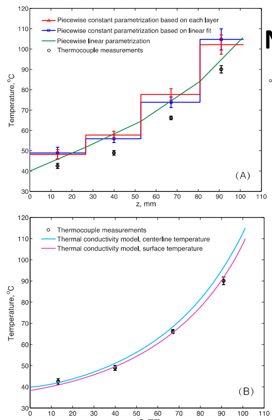

- Piecewise constant
- Piecewise linear
- 2D thermal model

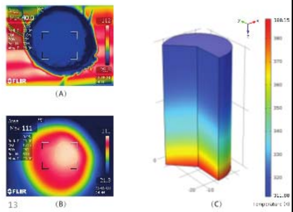

13

High Temperature Experiments

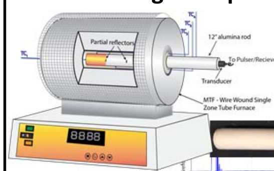

- Heated by tube furnaces
- Temperatures changed in 50C increments from 50 to 1150C

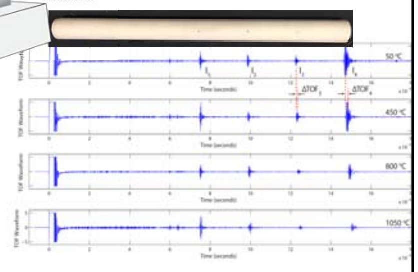

SOS vs. Temperature Calibration Curve

- Strong dependence on temperature
- 75% of measured temperatures have STD ± 1°C

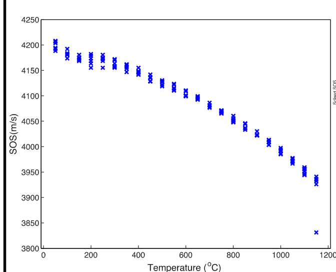

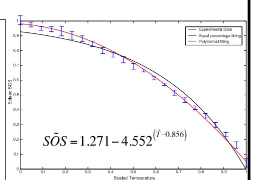

$$\tilde{SOS} = 1.271 - 4.552^{(\tilde{T} - 0.856)}$$

Equal percentage fit:

$$\tilde{SOS} = a - R^{(\tilde{T} - b)}$$

$$\tilde{SOS} = \frac{SOS - SOS_{min}}{SOS_{max} - SOS_{min}} \qquad \tilde{T} = \frac{T - T_{min}}{T_{max} - T_{min}}$$

15

SOS and Young’s modulus

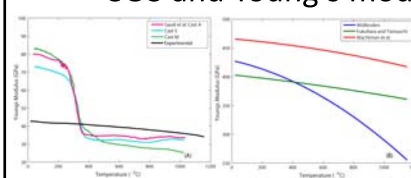

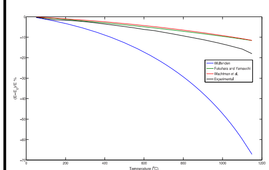

For p-waves:

$$C_p = \sqrt{\frac{K + \frac{4}{3}G}{\rho}} = \sqrt{\frac{E(1-\nu)}{\rho(1+\nu)(1-2\nu)}}$$

For p-waves in long rods:

$$C_{rod} = \sqrt{\frac{E}{\rho}}$$

16

Comparison with TC Measurements: Steady State and Dynamic Temperature

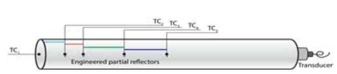

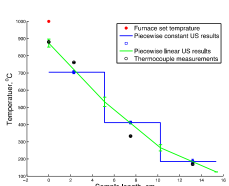

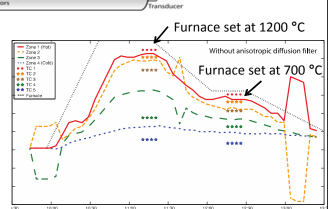

17

Envelope timing: Still not good enough

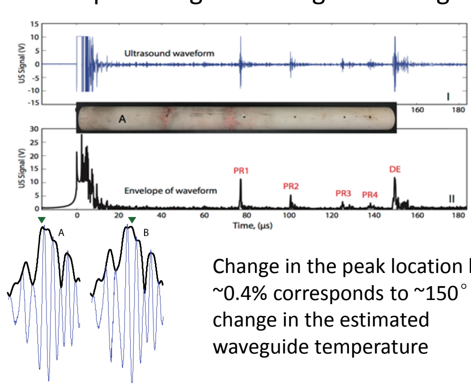

Change in the peak location by ~0.4% corresponds to ~150° C change in the estimated waveguide temperature

Anisotropic Diffusion (Perona-Malik) Filter

Iteratively filter images using diffusion operator with spatially varying diffusion coefficient:

$$\frac{\partial}{\partial \tau} u(\mathbf{r},\tau) = \nabla \cdot \left[(D(\mathbf{r},\tau) \nabla u(\mathbf{r},\tau) \right], \quad u(\mathbf{r},0) = I(\mathbf{r})$$

Common choices of D

Preserves high-contrast edges — Favors wide regions

$$D_1(\mathbf{r},t) = \exp\left(-\left(\frac{|\nabla I(\mathbf{r},\tau)|}{\kappa} \right)^2 \right) \qquad D_2(\mathbf{r},t) = \frac{1}{1 + \left(\frac{|\nabla I(\mathbf{r},t)|}{\kappa} \right)^{1+\alpha}}, \quad \alpha > 0$$

κ: gradient modulus threshold for conduction control

Anisotropic Diffusion Using in Image Processing

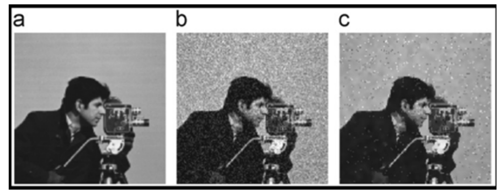

a: Original image
b: Original plus Gaussian noise (σ=0.1)
c: Filtered by anisotropic diffusion after 15 iterations.

C. Tsiotsios and M. Petrou, "On the choice of the parameters for anisotropic diffusion in image processing," Pattern recognition, vol. 46, no. 5, pp. 1369–1381, 2013.

1D Anisotropic Diffusion applied to envelope

$$\frac{\partial}{\partial \tau} u(t,\tau) = \frac{\partial}{\partial t}\left[D(t,\tau) \cdot \frac{\partial}{\partial t} u(t,\tau) \right]$$

$$\approx \frac{\left[D(t+\frac{\Delta t}{2},\tau) \cdot (u(t+\Delta t,\tau) - u(t,\tau)) - D(t-\frac{\Delta t}{2},\tau) \cdot (u(t,\tau) - u(t-\Delta t,\tau)) \right]}{\Delta t^2}$$

where

$$D(t+\frac{\Delta t}{2},\tau) = \exp\left(-\left(\frac{(u(t+\Delta t,\tau) - u(t,\tau))}{(\kappa \Delta t)^2} \right)^2 \right)$$

$$D(t-\frac{\Delta t}{2},\tau) = \exp\left(-\left(\frac{(u(t,\tau) - u(t-\Delta t,\tau))}{(\kappa \Delta t)^2} \right)^2 \right)$$

Starting with the original envelope, $u(t,0) = A(t)$,iterate to update the filtered values

$$u(t,\tau+\Delta\tau) = u(t,\tau) + \Delta\tau \cdot rhs$$

Application of Anisotropic Diffusion Filter

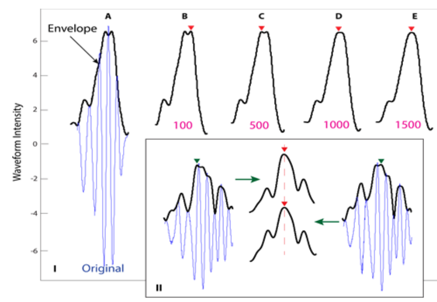

22

Comparison of TOF timing errors

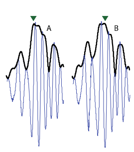

TOF Estimation Methods	Cementitious Sample, TOF Differences (ns)	Alumina Sample, TOF Differences (ns)
Peak of the waveform	90	30
Threshold of the waveform	100	25
Waveform Cross-correlation	72	26
Envelope Cross-correlation	56	26
Peak of filtered envelope	0	0
Cross-correlation of Filtered Envelope	0	0

Small TOF errors in TOF translate into large temperature errors: Alumina sample

TOF Estimation Methods	TOF Differences (ns)	Temperature Differences (20° C as reference) (° C)
Peak of the waveform	30	50.47
Threshold of the waveform	25	42.30
Waveform Cross-correlation	26	43.94
Envelope Cross-correlation	26	43.94
Peak of filtered envelope	0	0
Cross-correlation of Filtered Envelope	0	0

At 20 ° C:

- The average TOF of 2" alumina waveguide is 24.2 μs.
- A TOF measurement error by 0.1% implies that the temperature measurement error of 41 ° C.

Dynamic Temperature Measurements - Application of anisotropic filter

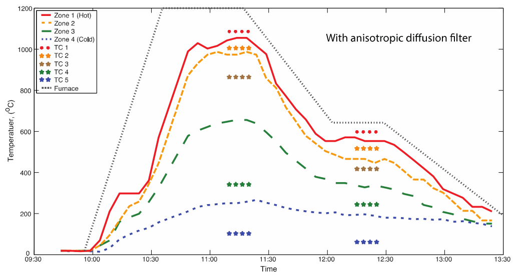

Pilot Scale Testing: Down-flow Oxy-fuel Combustor

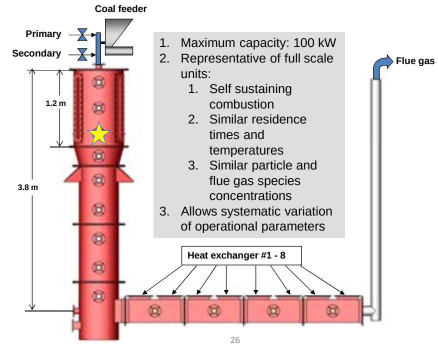

26

US Temperature Measurement System: Components

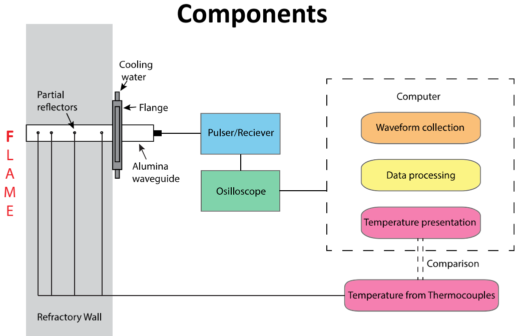

27

Mounting US waveguide

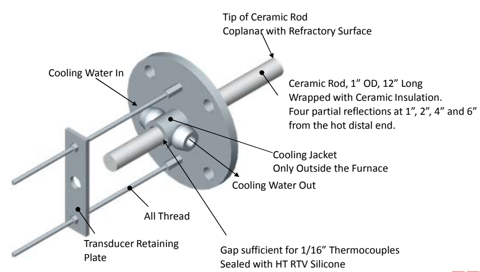

THE UNIVERSITY OF UTAH

28

US Measurement System: Installation

Natural Gas Preheating

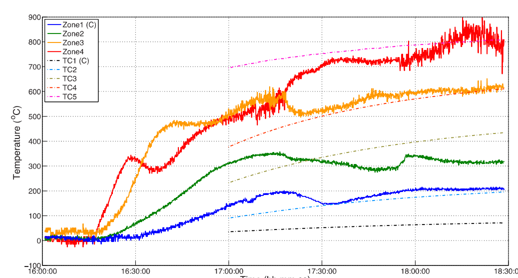

30

Stable NG Combustion

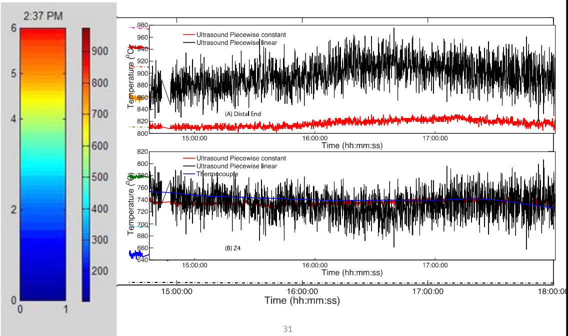

31

Transition from NG to Coal

32

Transition from NG to Coal

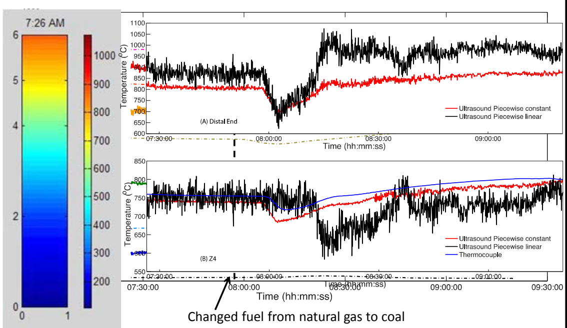

33

Coal Combustion with Coal Feed Rate Adjusted

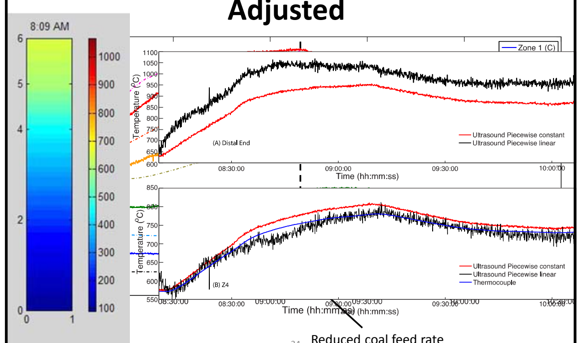

34

Stable Coal Combustion

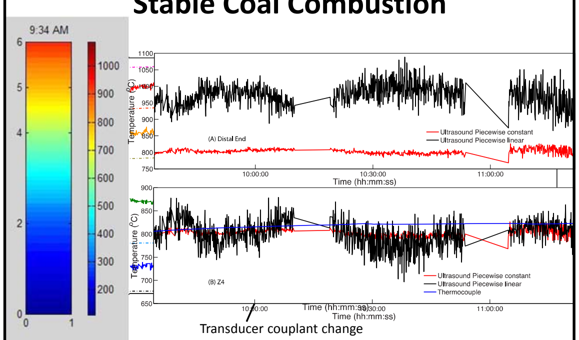

35

After Tests

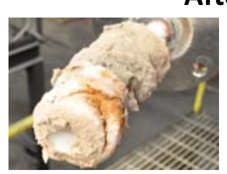

(Left) Ash deposition found on the ceramic insulation that covered the alumina rod. (Right) The alumina rod appears visually undamaged after the pilot scale test.

- Revealed issues
  - Continuous real-time monitoring will require permanent coupling between the transducer/receiver and the waveguide.

36

Grain growth

Significant deterioration of the ultrasound signal was observed after long time operation in high temperature condition.

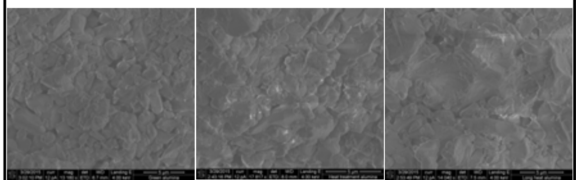

No heat treatment | Short heat treatment | Long heat treatment

Conclusions

- Noninvasive US measurements of temperature distribution in solids at extreme conditions are possible
- Can be used to measure conductive heat fluxes deep inside solids
- Pilot-scale tests shows that the method provides accurate continuous real-time in-situ measurements of temperature distribution across the containment. Real time temperature changes were captured during all relevant process changes.
- Temperature distribution can be measured in multiple locations
- Method can be used with existing and integrated into new units
- Broadly applicable in energy conversion applications
- Can be used to measure temperature distribution on a line, surface, or volume

Moving forward

- **Ready for early adoption and testing on industrial units**: Gasifiers, combustors, kilns, smelters, …
  - Can be used to measure temperature across multiple cross-sections of containments, nozzles, and other components.
  - New units can be designed to take better advantage of new capabilities for achieve better efficiencies, flex-fuel capabilities, longer service life
- **LOOKING FOR COMMERCIALIZATION PARTNERS**

- Broadly applicable in energy, chemical, military, space, and other applications with extreme conditions
- Environment does not have to be "extreme"
- Temperature distributions on a line, surface, or volume can be measured!
- Micro- and nano-scale applications

Team

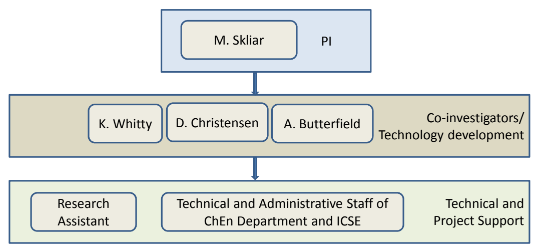

Graduate Research Assistant: Yunlu Jia
Undergraduate Research Assistant: Colin Young, Nathan Yonkee
High School Research Assistant: Melissa Puga
Graduate Research Consultant: Pál Tóth

Acknowledgements

- Funding by the U.S. Department of Energy National Energy Technology Laboratory, Grant DEFG2611FE0006947.
- Project manager: Barbara Carney

THE UNIVERSITY OF UTAH

References

1. Bennett, J.P., Kyei-Sing, K., "Refractory Liner Materials used in Slagging Gasifiers," *Refractory Applications and News*, 9: 20-25, 2004.
2. Dogan, C.P., Kwong, K.-S., Bennett, J.P. and Chinn, R.E. "Improved Refractories for Slagging Gasifiers in IGCC Power Systems", DOE Report 835687.
3. Hornick, M.J. McDaniel, J.E., "Tampa Electric Integrated Gasification Combined-Cycle Project," Final technical report for project under Cooperative Agreement DE-FC-21-91MC27363, 2002.
4. Liu, J.T.C., Rieker, G.B., Jeffries, J.B., Hanson, R.K., Gruber, M.R., Carter, C.D. and Mathur, T., "Near infrared Diode Laser Absorption Diagnostic for Temperature and Water Vapor in a Scramjet Combustor," Applied Optics, 44: 6701-6711, 2006.
5. Muzio L.J., Eskinazi, D., Green, S., "Acoustic pyrometry: new boiler diagnostic tool," J. Power Engineering, 12:32-37, 1989.
6. Green, S.F., "An acoustic technique for rapid temperature distribution measurements," J. Acoustical Society of America, 77: 765-769, 1985.
7. Bramanti, M., Tonazzini, A., Tonazzini, A., "An acoustic pyrometer system for tomographic thermal imaging in power plant boilers, " IEEE Trans. Instrumentation and Measurement, 45:87-94, 1996 .
8. Lu, J., Takahashi, S., Takahashi, S., "Acoustic computer tomographic pyrometry for two-dimensional measurement of gases taking into account the effect of refraction of sound wave paths," Measurement Science and Technology, 11: 692-697, 2000.
9. Lee, Y.J., Khuri-Yakub, B.T., Saraswat, K., "Temperature measurement in rapid thermal processing using the acoustic temperature sensor," IEEE Trans. Semiconductor Manufacturing, 9: 115-121, 1996.
10. Arthur, R.M., Trobaugh, J.V., Straube, W.L., Moros, E.G., "Temperature dependence of ultrasonic backscattered energy in motion compensated images," IEEE Trans. Ultrasonics, Ferroelectric and Frequency Control, 52:1644 – 1652, 2005.
11. M. Skliar, K. Whitty, and A. Butterfireld, "Ultrasonic temperature measurement device," PCT patent application, Pub. No: WO/2011/088393, International Application No: PCT/US2011/021396, 2011.
12. Y. Jia and M. Skliar, "Ultrasound measurements of temperature profile across gasifier refractories," Proposal to present at the Annual AIChE Meeting, November, 2012.
13. Y. Jia, Melissa Puga, A. Butterfield, D. Christensen, K. Whitty, and M. Skliar "Ultrasound Measurements of Temperature Profile Across Gasifier Refractories: Method and Initial Validation," *Energy & Fuels* 27.8 (2013): 4270-4277.
14. Y. Jia and M. Skliar, "Anisotropic diffusion filter for robust timing of ultrasound echoes," 2014 IEEE International Ultrasonics Symposium (IUS), Chicago, Il, pp. 560--563, 3-6 Sept. 2014.
15. Y. Jia and M. Skliar, "Ultrasound Measurements of Temperature Distribution and Heat Fluxes in Solids," Sensors and Actuators: A, submitted.

Thank you!

43

THE UNIVERSITY OF UTAH